The DiPOLE project: towards high energy, high repetition rate diode pumped lasers

Contact *klaus.ertel@stfc.ac.uk*

Klaus Ertel, Saumyabrata Banerjee, Paul Mason, Jonathan Phillips, Phil Rice, Steph Tomlinson, Christian Sawyer, Steve Blake, Cristina Hernandez-Gomez, John Collier
Central Laser Facility, STFC Rutherford Appleton Laboratory, Chilton, Didcot, OX11 0QX, UK

Tristan Davenne, Michael Fitton, John Hill, Andrew Lintern
Engineering Technology Centre, STFC Rutherford Appleton Laboratory, Chilton, Didcot, OX11 0QX, UK

Introduction

DiPOLE stands for Diode Pumped Optical Laser for Experiments. It is a new project at the CLF to develop the foundations of novel high energy, high average power laser systems based on diode pumped solid state laser (DPSSL) technology. Compared to conventional systems, this approach promises dramatically increased repetition rates (and hence average powers) at significantly higher electrical-to-optical conversion efficiency. DiPOLE has been included as an emerging opportunity in the Research Councils UK Large Facilities Roadmap [1].

Motivation

Laser amplifiers capable of producing energetic ns-pulses are one of the main tools for laser plasma research and high-energy applications. Laser chains containing such amplifiers can produce ns-pulses or ps-pulses if the chirped pulse amplification (CPA) technique is used. Depending on the application, these pulses are either applied directly or are used to pump other amplifiers (e.g. Ti:Sapphire or OPCPA) in order to obtain even shorter pulses in the fs-regime.

Currently, ns-amplifiers are based on flashlamp-pumped Nd:glass technology and their repetition rate is limited to a few shots per minute for amplifiers delivering tens of joules of pulse energy to a few shots per day for lasers delivering kJ-level pulse energies.

Increasing the repetition rate of such laser systems to the multi-Hz level (typically 10 Hz) is pivotal for the following applications:

- Opening up new horizons in fundamental laser plasma interaction research by enabling higher throughput and the exploration of larger parameter spaces.
- So-called secondary sources which use laser-generated plasmas to produce ultra-short pulses of energetic particles (electrons or ions) or electromagnetic radiation (ranging from THz to hard X-ray). High repetition rate drive lasers are required to generate sufficiently high particle and photon numbers. Much of the pan-European ELI project focuses on the development and exploitation of secondary sources [2].
- Inertial confinement fusion (ICF), which is expected to be demonstrated for the first time within the next two years. Whereas current low-repetition rate facilities like NIF and LMJ are suitable for proof of principle experiments, high-efficiency, high repetition rate DPSSL based laser drivers open up the possibility to develop ICF into a reasonably clean, practically inexhaustible source of energy. This is the focus of the pan-European HiPER project [3].

Amplifier concept

The main activity within DiPOLE is the development of a DPSSL amplifier concept that is capable of delivering kJ-level pulses at 10 Hz repetition rate.

Gain material selection

The starting point was the identification of the most suitable gain material. This material needs to provide:

- A long fluorescence lifetime to minimise the number of pump diodes required
- Good thermo-mechanical properties to handle the high average power
- Reasonably high gain cross section to enable uncomplicated and efficient energy extraction
- The possibility to be manufactured in large sizes to handle the high pulse energy.

Ytterbium (Yb) as an active laser ion offers very long fluorescence lifetimes, a low quantum defect (pump wavelength 940 nm, laser wavelength 1030 nm), reasonable gain cross sections and efficient high power laser diodes are readily available for its pump wavelength. Two host materials have been identified that offer good thermo-mechanical properties and can be manufactured in large sizes: crystalline calcium fluoride (CAF) and ceramic YAG.

Yb:CAF has a very long fluorescence lifetime of 2.4 ms and a large gain bandwidth (> 50 nm) [4], and is therefore a promising candidate for directly diode pumped chirped pulse amplification (CPA) systems for producing sub-ps pulses [5]. However, since it exhibits a very small gain cross section, very large fluence levels are required for both pumping and extraction in order to achieve good optical-to-optical (o-o) efficiency.

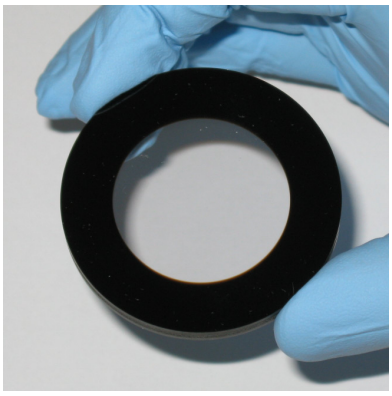

Fig. 1: Yb:YAG - Cr^{4+}:YAG compound disk.

On the other hand, Yb:YAG has an order of magnitude higher gain cross section with a reasonable fluorescence lifetime of 1 ms [6]. Since the main application of our envisioned kJ-class laser is the production of ns-pulses, either for pumping amplifiers for fs-pulse generation (Ti:sapphire or OPCPA) or for driving inertial fusion targets, we think that ceramic Yb:YAG is the best choice for the gain medium. Also, monolithic compound structures with different doping species are possible with ceramic YAG [7]. The photo of such a

compound disk is shown in Fig. 1. Here the inner region of the disk is doped with Yb^{3+} and acts as the active laser medium, the outer region is doped with Cr^{4+} which heavily absorbs at 1030 nm and therefore acts as an index-matched absorber for suppression of amplified spontaneous emission (ASE) [8].

Efficiency and gain modelling

Numerical modelling has been carried out to determine optimum amplifier design parameters. In the model, the storage efficiency η_{stor} has been calculated for various parameters like pump fluence, pump pulse duration and pump spectral width. η_{stor} is defined as extractable fluence divided by pump fluence. Loss mechanisms and associated efficiency factors that influence η_{stor} are: η_{fluo} for the fluorescence decay, η_{QD} for the quantum defect, η_{abs} for pump light that passes through the gain medium without being absorbed and, finally, η_{reabs} for the minimum upper state population that needs to be established in order to overcome reabsorption that exists due to the quasi-3-level nature of Yb:YAG. If a pump pulse duration of 1 ms is chosen, η_{QD} and η_{fluo} limit η_{stor} to 58 %. It turns out that η_{abs} and η_{reabs} need to be balanced off against each other and that for a given set of pump-related parameters, there is one optimum value for gain medium optical depth (OD = thickness times doping concentration) that yields the maximum η_{stor}. If OD is chosen too low, too little pump light is absorbed, if OD is too high, reabsorption losses become dominant.

The following results are calculated, unless stated otherwise, for an amplifier that is end-pumped from both sides with a pump pulse duration of 1 ms, a 5 nm FWHM pump spectral width, centred at the optimum wavelength in the 940 nm absorption band. Spectrally resolved pump absorption cross sections were taken from [9]. Quantities calculated were η_{stor} and the small signal gain G, defined as $G = \exp(\eta_{stor} F_{pump}/F_{sat})$ where $\eta_{stor} F_{pump}$ is the extractable fluence and F_{sat} the gain saturation fluence. First, calculations were carried out for room temperature operation. The results are shown Fig. 2. It becomes apparent that very strong pumping is required, firstly to overcome the high reabsorption losses and to achieve good efficiency and secondly to overcome the still rather low gain cross section and achieve reasonable gain. The required high pump and extraction fluences are difficult to achieve because of limited pump source brightness and limited laser damage threshold.

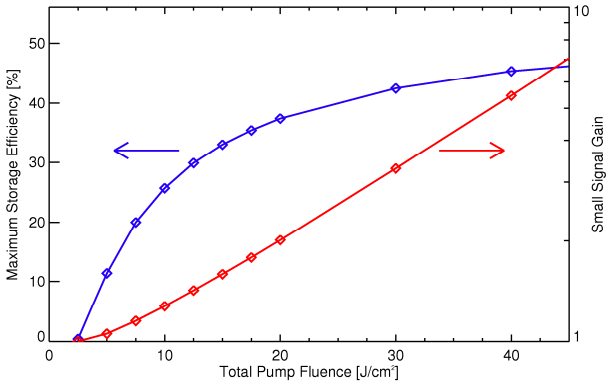

Fig. 2: Maximum storage efficiency (blue) and small signal gain (red) for amplifier operated at room temperature.

Cooling the gain medium to 175 K drastically changes the situation, as illustrated in Fig. 3. Reabsorption is reduced and the gain cross section increased, leading to greatly improved efficiency and gain, especially at moderate fluences. A pump fluence that is realistically achievable with today's laser diodes is 10 J/cm^2 (5 J/cm^2 from each side), yielding a storage efficiency of just over 50 % (resulting in an extractable fluence of 5 J/cm^2) and a small signal gain of 3.8. This fluence is therefore chosen as the preliminary operating point for our amplifier.

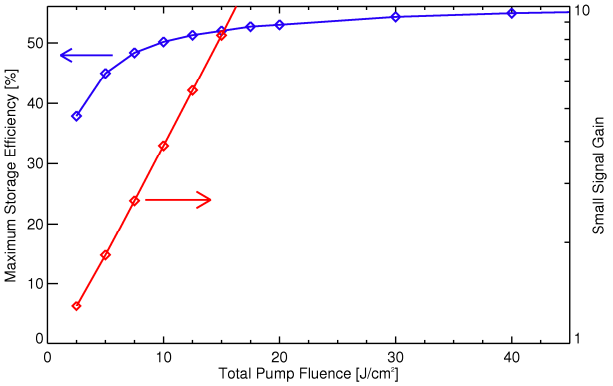

Fig. 3: Maximum storage efficiency (blue) and small signal gain (red) for amplifier operated at 175 K.

Operating at cryogenic temperatures yields the added benefit of improved thermo-mechanical and thermo-optical properties like increased thermal conductivity and reduced temperature dependence of the refractive index [10]. Another effect is the narrowing of spectral features both in the emission and the absorption spectrum. The absorption spectra measured at room temperature and at 175 K are shown Fig. 4, together with a 5 nm FWHM Gaussian spectrum for comparison, which is assumed to be the spectral shape of our pump source.

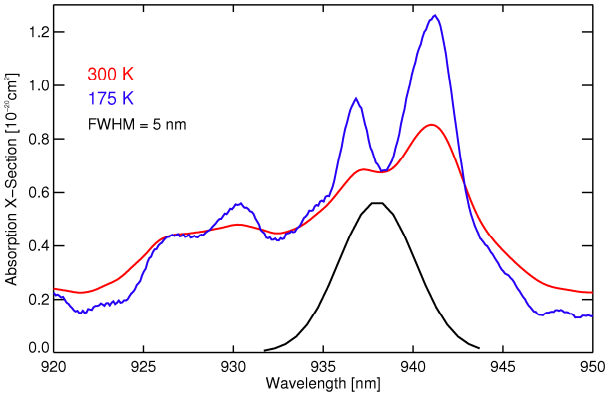

Fig. 4: Absorption spectra of Yb:YAG at different temperatures and 5 nm wide pump diode spectrum for comparison.

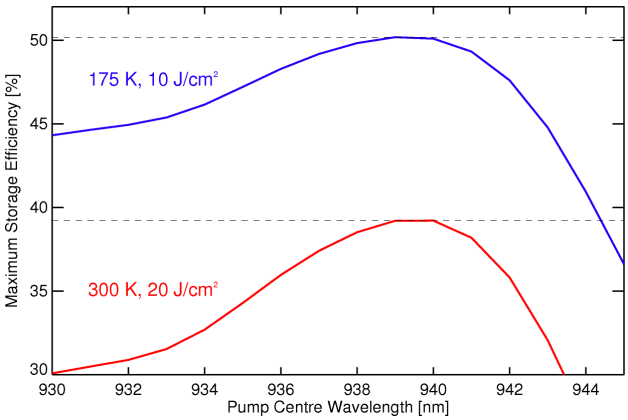

Fig. 5: Storage efficiency as function of pump centre wavelength for two different temperatures and pump fluences.

If these pump and absorption spectra are used to calculate storage efficiency for two different temperature scenarios, results as shown in Fig. 5 are obtained. Even though the pump fluence in the low temperature scenario is only half that of the room temperature case, significantly higher storage efficiency is predicted. Lower temperature operation also shows a much

weaker dependence on pump centre wavelength. So despite narrower absorption features, the requirements with respect to spectral performance of the pump diodes are less critical for low temperature operation.

Amplifier geometry

After determining operating temperature and pump fluence for our envisioned amplifier, the actual geometry needs to be defined. If the laser system is to yield an output energy of 1 kJ and the amplifier is to be operated at an output fluence of 5 J/cm^2, the aperture needs to be 200 cm^2 or 14 x 14 cm^2 if a square beam shape is adopted. The optimum OD = *N*x*l* obtained from the numerical calculations is 3.15 % cm, where *N* is the Yb-doping concentration in atomic % and *l* the geometrical thickness of the amplifier. The choice of *N* and consequently *l* is governed by ASE management considerations. If the gain-length product along the diagonal across the (square) surface of the amplifier is to be kept below 3, we require $N < 0.18$ % and hence $l > 18$ cm. Such a thick amplifier requires distributed cooling as demonstrated on the Mercury laser [11]. There, the gain medium is divided into a stack of thin slabs with He gas flowing through the gaps between the slabs. The concept is illustrated in Fig. 6, where an amplifier consisting of 10 slabs is shown.

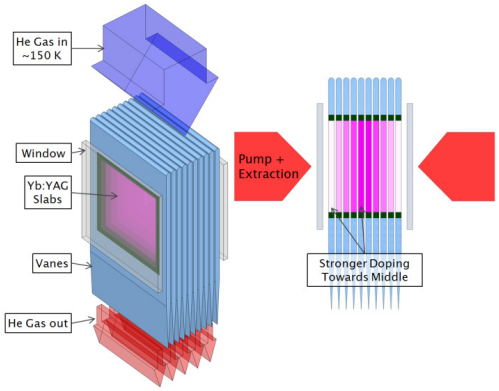

Fig. 6: Illustration of amplifier geometry: isometric (left) and side view (right).

If the criterion that the transverse gain-length product must not exceed a certain value is applied to each individual slab, one realises that the doping concentration can be increased towards the centre of the amplifier. The advantage is twofold: firstly, since the required overall OD remains the same, the amplifier as a whole becomes thinner, saving material and reducing the impact of nonlinear effects, and secondly the optical power absorbed in the individual slabs and hence the heat load is equalised. An optimised doping profile for a 10-slab amplifier is shown in Fig 7, together with the transverse gain as a function of position. The overall thickness of the gain medium is reduced from 18 cm to 10 cm in this configuration.

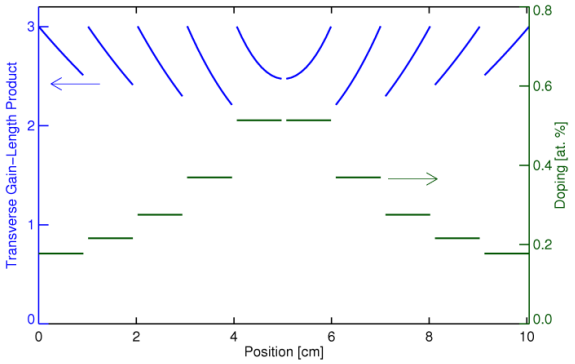

Fig. 7: Transverse gain-length product and doping levels along optical axis in 10-slab amplifier.

DiPOLE prototype

To test the concept in the laboratory a lower-energy multi-J prototype amplifier system is currently being built. The design is based on four co-sintered ceramic YAG discs (55 mm in diameter x 5 mm thick) where the Yb-doped region (35 mm diameter) is surrounded by a 10 mm thick Cr^{4+} cladding to absorb unwanted transverse fluorescence. A photograph of one of these discs is shown in Fig. 1. Given the 2 cm total gain medium thickness, two different Yb doping levels of 1.1 and 2.0 atomic% have been chosen to maximise storage efficiency and to equalise the heat loading. The discs are mounted in a vacuum insulated pressure vessel through which cryogenically cooled He gas is flowed. A schematic of the cryocooler system is shown in Fig. 8. The amplifier is end-pumped from both sides by two diode pump lasers operating near 940 nm. Each source provides 20 kW peak power in pulses of ~1 ms duration in a square beam (2 x 2 cm^2), with a corresponding pump intensity of 5kW/cm^2 and at a repetition rate of 10 Hz.

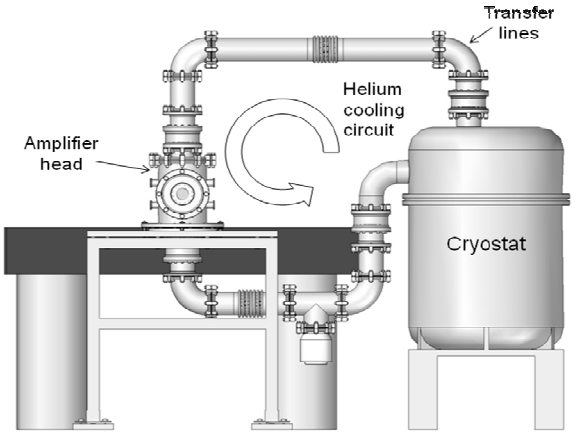

Fig. 8: Schematic diagram of the cryocooler system under development at CLF.

Conclusions

In summary, we have presented the conceptual design of a cryogenic Yb:YAG amplifier that can be scaled to kJ energy levels and beyond, owing to its geometry and unique cooling technique. Considerable enhancement in optical-to-optical conversion efficiency is predicted with the reduction of pump fluence at low temperatures owing to the reduced reabsorption losses, increased pump adsorption and gain cross sections. Numerical modelling also shows a weaker dependence on pump centre wavelength at low temperature, relaxing the stringent requirements of the diode pump source. The introduction of doping gradient in the slab architecture helps facilitate a uniform gain distribution and heat load in addition to the reduction of the overall thickness of the amplifier medium from 18 cm to 10 cm. A lower-energy multi-J prototype amplifier system is currently under development at CLF as a proof of principle.

References

1. Research Councils UK Large Facilities Roadmap, http://www.rcuk.ac.uk/research/resinfra/lfroadmap.htm.
2. The Extreme Light Infrastructure (ELI) European Project, http://www.extreme-light-infrastructure.eu/.
3. HiPER project, http://www.hiper-laser.org/.
4. P. Camy et al, "Comparative spectroscopic and laser properties of Yb^{3+}-doped CaF_2, SrF_2 and BaF_2 single crystals," Appl. Phys. B **89**, 539–542 (2007).
5. M. Siebold et al, "Terawatt diode-pumped Yb:CaF_2 laser," Opt. Lett. **33,** 2770-2772 (2008).

6. T. Taira, "RE^{3+}-Ion-Doped YAG Ceramic Lasers," IEEE J. Sel. Top. Quant. **13**, 798-809 (2007).

7. H. Yagi, " $Y_3A_{l5}O_{12}$ ceramic absorbers for the suppression of parasitic oscillation in high-power Nd:YAG lasers, " J. Luminescence **121**, 88-94 (2006).

8. K. Ertel et al, "ASE suppression in a high energy titanium sapphire amplifier," Opt. Express **16**, 8039-8049 (2008).

9. D. C. Brown et al, "Yb:YAG absorption at ambient and cryogenic temperatures, " IEEE J. Sel. Top. Quant. **11**, 604-612 (2007).

10. T. Y. Fan et al, "Cryogenic Yb^{3+}-doped solid-state lasers," IEEE J. Sel. Top. Quant. **13**, 448-459 (2007).

11. A. Bayramian et al, "The mercury project: A high average power, gas-cooled laser for inertial fusion energy development," Fusion Sci. Technol. **52**, 383-387 (2007).

Timing and Synchronisation System Designs for the New Light Source

Contact *Graeme.Hirst@stfc.ac.uk*

G. J. Hirst

STFC Central Laser Facility
Rutherford Appleton Laboratory, HSIC, Didcot OX11 0QX, UK

Introduction

The New Light Source (NLS) [1] was a proposed UK and international user facility based around a combination of Free Electron Lasers (FELs) and conventional lasers. In 2009 it was decided to halt work on the proposal once the Conceptual Design Report had been completed. Among the subsystems described in the CDR[1] was a sophisticated laser-based timing and synchronisation network, designed by CLF staff.

The NLS was designed to support a very wide range of science, a significant fraction of which exploited its ultrashort pulse capabilities and, in particular, its ability to deliver several beams to an experiment simultaneously. The relative timing of the pulses in these beams had to be tightly managed, either to overlap them reliably in time, e.g. for multiphoton experiments, or to provide them with variable relative delay(s) e.g. for pump-probe studies. In addition to the lasers delivering beams directly to users there were also lasers acting as components of the NLS machine itself. The timing of the pulses from these needed to be controlled to ensure that the facility functioned at all. This article describes the systems used to manage the timing and considers the performance of an example subsystem in more detail.

Time Structure

The NLS time structure was decided in consultation with the scientific user community. The outcome was particularly simple, driven by a strong preference for the pulses from each FEL and laser to be delivered in a continuous, evenly-spaced, high-rate train. (Experiments needing a lower rate would have the option of pulse selection.) As far as the timing was concerned the only parameters to be decided were, therefore, the pulse duration and repetition rate. The duration was chosen to be 20 fs FWHM to allow the best possible time resolution. There was a clear science requirement for an initial rate of at least 1 kHz with an upgrade path that would increase this, in approximately decade steps, to 1 MHz. In principle exactly these rates could have been chosen. But in fact slightly different rates were selected with a view to minimising the timing jitter of the resulting pulses.

The starting point for the rate was the frequency of the RF modules which accelerated the electrons for the FELs. This was predetermined by industry standards to be 1.300 GHz. The NLS operating rate would need to be an integer sub-multiple of this and for technical reasons the timing jitter would be minimised if the integer chosen had only very small integer factors itself (ideally only 2 and 3). The eventual scheme is shown in Fig. 1. The overall master clock frequency was chosen to be 216.67 MHz, the sixth harmonic of which would generate the 1.3 GHz RF. The nominal 1 kHz pulse rate to be delivered on Day 1 of operations was actually 1.102 kHz (1.3 GHz divided by $2^{17} \times 3^2$). Subsequent upgrades would increase it by factors of 2^3, $2^2 \times 3$ and 2^3, eventually reaching 0.846 MHz. An additional feature of this choice was that the rate after each upgrade would be an integer multiple of the rate before. This would make it easier for legacy systems to remain operable after any upgrade.

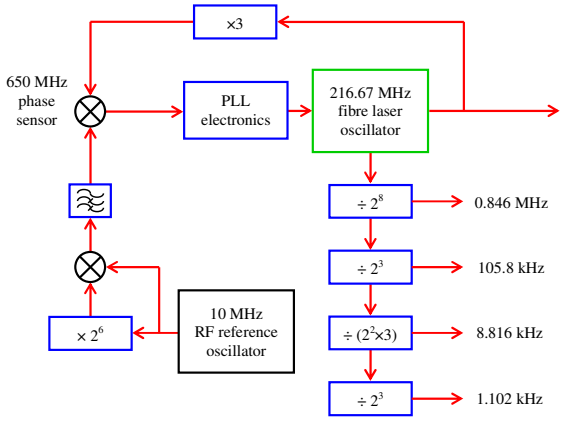

Figure 1. NLS master clock architecture showing pulse rate division scheme.

Synchronisation

The potential that ultrashort pulses offer for very high temporal resolution and also for high-intensity multiphoton science can only be achieved if the relative pulse timing is very tightly managed. For a subset of NLS experiments it would be sufficient if the timing management consisted simply of pulse-by-pulse timing measurement followed by time-stamping of the resulting data. However there were also experiments for which this approach would not be adequate and, in particular, there were aspects of the machine operation (for example the use of conventional lasers to seed the FELs) where the timing would need to be *controlled* rather than just measured. For this reason a synchronisation control system was designed which would be deployed across the whole of the NLS.

Given the 20 fs FWHM chosen pulse length, the target figure for *overall* synchronisation was set at 10 fs RMS. This was recognized as a challenge since individual subsystems have only been developed to this level of performance in recent years. However the NLS would have an advantage over almost all similar facilities in that it would be built from scratch without having to accommodate any pre-existing hardware or design decisions. This would allow the need for low timing jitter to be factored into the design from the start.

The entire synchronisation system is too complex to describe here. Instead the general approach will be illustrated by an example. One of the features of the NLS was the configuration of its FELs as seeded amplifiers with the seed pulses derived by high harmonic generation from conventional lasers. The timing of the FEL pulses would then be set by the timing of the seed lasers and the stability of the output beam transport paths. This scheme imposes two separate synchronisation requirements. Firstly that the seed pulses must overlap the electron bunches in the FEL undulator. The nature of electron accelerators, whose transport systems are inherently dispersive, makes this difficult to achieve. The fact that the NLS accelerator did achieve it[2] is testament to the very considerable effort and creativity of the design team. But the bulk of that work concerned the accelerator itself rather than the synchronisation system and it will therefore not be discussed further here.

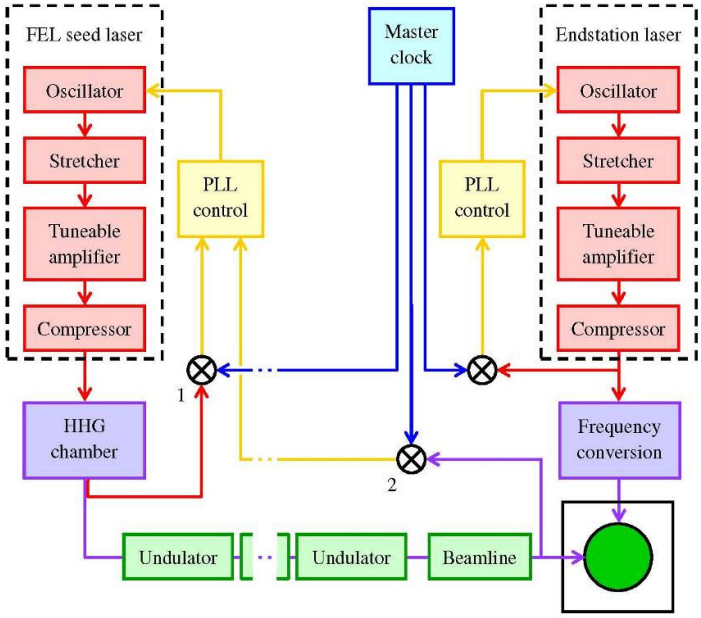

Figure 2. Layout of the elements used to synchronise FEL and laser pulses at the users' experiments. 1 and 2 represent the first and second phase sensors for the FEL seed laser.

The second challenge is the delivery of the FEL pulses to the users' experiments in exact synchronism with pulses from a conventional "endstation" laser. The scheme devised to do this is shown in Fig. 2. The physical scale of the system is large - the seed laser and the endstation laser are more than 100 m apart. Yet the need for less than 10 fs timing jitter corresponds to a relative movement of the pulses in space of less than 3 μm. So issues around the transport of beams and of timing signals are critical. For this reason a master clock architecture was chosen (the details of the low-noise clock are shown in Fig.1). The alternative would have been to use a common laser oscillator and to split the beam from this to feed the two amplifier chains. The first problem with this is that transporting ultrashort pulses over long distances is difficult. To avoid nonlinear effects the transport has to be in free-space (ideally in vacuum) using curved mirrors for image-relaying to preserve the beam quality. Engineering such a system for high stability would be very expensive. On the other hand the technology needed to transport optical clock pulses with few-femtosecond jitter has already been developed and demonstrated[3].

The second problem with a common oscillator is that the active control system needed to correct the pulse timing in real time ideally uses the position of an oscillator cavity mirror as its actuator. Such a mirror is multi-passed very many times on the timescale of the correction signal (typically >10 μs). So the mirror need only be moved a tiny distance, which eases high speed operation. Of course if there was only one oscillator then movement of its mirrors would not correct the *relative* timing of the endstation laser and FEL pulses. So an extra-cavity actuator would have to be used which would be less effective.

Having distributed accurate clock signals to the phase (timing) sensors in Fig. 2, the next task is to reduce the timing error they detect using a closed phase-locked loop (PLL). Again this is a well-established technique and locking of a laser oscillator to an external reference using optical phase sensing has also been demonstrated at the femtosecond level[4]. Extending this technique to include the laser amplifier chain inside the timing control loop should be straightforward, the only complication being the reduction in pulse rate relative to the oscillator. This imposes a Nyquist limit on the phase noise spectrum which can be sensed. However given that the lasers are designed to operate at up to 1 MHz it seems likely that this limit will be higher than the one imposed by the correction actuators.

Once the seed laser is phase-locked FEL action can begin and the opportunity then exists to correct timing jitter arising in the FEL and beam transport paths. This will involve sensing the pulse timing after the FEL, at point 2 in Fig. 2. This will be considerably more challenging than sensing the laser timing a) because phase sensing in the EUV, where the FEL operates, is not yet a mature technology, b) because the FEL will be tuned over a much wider photon energy range than the laser and c) because the uncorrected noise levels (both amplitude and phase) from the FEL will be higher than for the laser systems alone. The effectiveness of the correction system depends directly on these levels. However despite these problems a post-FEL correction scheme has been included in the design as it promises the easiest route to reaching the overall jitter target. The tuning issue will also apply to the endstation laser if it proves necessary to stabilise its timing after its nonlinear frequency conversion. The initial plan is to achieve stability passively, by mounting the converters close to the endstation and in a well-controlled environment. But the option of active stabilisation has not been discounted.

Conclusions and Acknowledgement

Some elements of the timing and synchronisation scheme for the NLS have been described. The timing is expected to be straightforward. Delivering 10 fs RMS overall synchronism will be challenging, but it should be achievable using state of the art subsystems. This work was partly supported by "IRUVX-PP", an EU co-funded project under FP7 (Grant Agreement 211285).

References

1. J. Marangos et al, *NLS Project: Conceptual Design Report*, publ. STFC (2010)
2. R. Bartolini, *Optimisation of a single-pass superconducting linac as a FEL driver for the NLS project*, Paper WEOB02, 31st International FEL Conference, Liverpool, UK (2009)
3. J. Kim et al, *Long-term femtosecond timing link stabilization using a single-crystal balanced cross correlator*, Opt Letts **32** (9) 1044 (2007)
4. See e.g. T. R. Schibli et al, *Attosecond active synchronization of passively mode-locked lasers by balanced cross-correlation*, Opt Letts **28** (11) 947 (2003)

Experimental setup in the Vulcan HaPPIE Laboratory for Multi-beam Combination to achieve Diffraction limit pulses

Contact *jonathan.phillips@stfc.ac.uk*

P.J. Phillips, C. Hernandez-Gomez, J. Collier

CLF, Science and Technology Facilities Council
Rutherford Appleton Laboratory
Harwell Science and Innovation Campus
Didcot
OX11 0QX

Introduction

High powered lasers are attractive owing to their potential for a diverse range of experiments. In order to achieve these high powered lasers, various choices for amplification of laser beam have to be made. These choices include the size of the beam which in turn requires laser crystals or ceramics to be manufactured close to their current limit of scalability. Another way of achieving these high power requirements is to combine several beams into a monolithic beam, which immediately reduces the requirements for the amplifier to a more modest level. This requires technology to lock the beams spatially and temporally.

A number of projects are underway in Europe under the umbrella of the LASERLAB-EUROPE II to research high power laser beams. There are several initiatives under this known as Joint Research Areas (JRA) of which one of them is the **H**igh **A**verage and **P**eak **P**ower lasers for **I**nteraction **E**xperiments (HAPPIE) to target the technology areas which are deemed useful to achieve high power lasers. One of these technology areas is the control of the spatial and temporal overlap of combining these beams in a coherent manner.

Specifically in the case of laser fusion project, known as HiPER[1] it is envisaged to include a fast ignition beam. This fast pulse ignition beam requires ~60 KJ with Picoseconds pulse width. This beam is to be composed of multiple subbeams in order to achieve the required power levels for fast ignition. A number of these subbeams will be combined to act as monolithic beam. This also reduces the requirements on the power from each individual amplifier stage and gives a level of control on the different subbeams for pulse shaping. In order for the laser power to achieve the diffraction limit at the interaction point, it requires that the subbeams be temporally and spatial overlapped. It is also currently thought that the main igniter beam would now also compose of subbeams.

Another pan European laser project called Extreme Light Interaction (ELI); which involves development and construction of three separate lasers in different geographical locations. It is currently thought that each laser will be constructed from several laser beams which also require spatial and temporal overlap.

Spatial overlapping can be achieved by several techniques[2]; most prominently this is achieved in the Large Telescopes either in use or currently being developed around the world. These large telescopes are constructed from segmented mirrors and the wavefront needs to be flattened to within a fraction of the wavelength to achieve the diffraction limit to fully exploit the capability of the telescope. We are currently setting up a laboratory to investigate the different techniques in wavefront measurement spatial and temporally.

Wavefront measurement methodologies

In the case of wavefront measurement there are several different methods which are employed. These methods traditional measure the wavefront of one aperture and correct this wavefront. The two most common methods is a Shack-Hartmann wavefront sensor and an interferometer based technique via the multiwave lateral shearing interferometer[4]. A Shack-Hartmann technique samples the wavefront with the use of a grid of microlenses which is focused onto a sensor, generally a CCD camera. In the case of a distorted wavefront the focused points on the CCD camera are misaligned relative to an undistorted wavefront which is proportional to the distortion in the wavefront. The position of focused spots compared to a set of reference focused points for a "perfect" wavefront is used create a phase map can be extracted of the measured wavefront or a Fourier demodulation technique, which obtains an error signal. The phase map for one aperture is generally expressed as a set of either Zernike or Legendre polynomials. Error signal can then be used to correct the wavefront by the use of an adaptive mirror. Adaptive mirror contains actuators to control the shape of the mirror so that the distortion can be corrected in the wavefront. In the case a multiwave lateral shearing interferometer uses a 2D diffraction grating which replicates the incident beam into 4 identical waves which are propagated along slightly different directions. These directions differences create inference patterns. After a few millimeters propagation the four beams are slightly separated. The grid deformations are directly connected to the phase gradients. A spectral analysis using Fourier transforms allows the phase gradient extraction in two orthogonal planes. The phase map is finally obtained by integration of these gradients. As explained in the case of Shack-Hartmann sensor the phase map can be used as an error signal to an adaptive mirror. These methods do not provide a piston error, this being the amount of lateral movement one beam has to make with the second beam so that they are spatial overlapped as they propagate, so cannot be used to spatial overlap two beams.

To create a phase difference between two independent sub apertures then it is important to interfere the two wavefronts. This then creates an interference pattern between the two wavefronts from the sub apertures and then the phase information (piston measurement) can be extracted. In order to obtain this piston measurement between two sub aperture beams then a quadriwave lateral shearing interferometer (QWLSI) [4] can be employed. This measurement is self referenced, which makes it easy to implement. This method adapts the well known multiwave lateral shearing interferometry used for wavefront sensing to phase difference evaluation by extending the shearing distance so that the edge of one subbeam overlaps the edge of another subbeam. Analysing the interference pattern in this overlap region leads to this phase difference between the two subbeams. One particular system designed to do this is the PHASICS camera SID4. This was developed in collaboration with the CEA CESTA who developed the system for the phasing of two LIL compressed beams[5]. The piston accuracy can be estimated to be 40 nm or less.

If we consider two beams with complex amplitude $A(B) = \sqrt{I_{A(B)}}\exp(j(\psi_{A(B)}) + c.c.$ then split the beam into a 4 wave interferometry. We get a case of independent subbeams, and to obtain the simplest beamlet combination, it is necessary to align the physical gap direction between the subbeams with the interferometer replication grating in axis y. In this case we obtain a situation similar to the 2-wave case. We observe 4-wave interferences, with the two wave interference zones at its left and right. The 4-wave interference zone labelled OR is illuminated by four replicas, A1, A3, B2 and B4. In the OR zone, the pattern results from the amplitude double product$(A_1B_2^* + A_3B_4^*)$. The argument of this sum leads to a phase difference that is equal to$[(\psi_{A1} + \psi_{A3}) - (\psi_{B2} + \psi_{B4})]/2 \approx \psi_A - \psi_B$. In the left (right) zone, the pattern results from the interference of replicas from the same initial beam A (B). The argument of the corresponding amplitude sum leads to A (B) beam phase gradient. Considering an unaberrated beam, this phase gradient should be equal to zero or to a constant if the wavefront is tilted. In the case of unaberrated beams a graph of the total amplitude argument versus x may represent a top hat shape where the amplitude, P(x), represents the phase difference between the two independent subbeams A and B. Futhermore, in the case of angularly phased subbeams, its amplitude would be equal to the piston difference between them. A deeper theoretical study shows that a deconvoluted signal in the overlap zone allows characterization of not only the piston but also tip and tilt and higher order aberrations.

Current Progress

Under the JRA there is a specific task that requires the development of novel metrology and techniques to lock a number of pulses of discreet test large apertures together through active phase control. These test apertures are of a small size so that any technical difficulties can be solved at this point in so that they can be scaled to a larger size required for current planned facilities. With this in mind at CLF we have developed a laboratory to asses various techniques for beam phasing experiments. The initial experiments will conducted in CW mode of a Ti:Sapphire laser output. A PHASICS camera is employed for capture and analysis of the combined wavefront. As shown in Figure 1 the optical layout expands the beam to a 120 mm beam from the laser, so that it can be subdivided into at maximum four beams of 50mm square. Although initially the experiment will start by using two beams of 50 mm square each. The two mirrors have independent control of tip / tilt and a translation stage for each mirror for piston control. Mirror 1 is the slave to Mirror 2 so that when a piston error is calculated by the PHASICS camera and software, this translation stage is aligned to bring the piston error close to zero. In Figure 1 the combined beam is relay imaged from the two square mirrors onto the PHASICS camera, to ensure that the plane of reference is imaged onto the focal plane array of the camera. The beam condenser system composes of a 570 mm lens and a 100 mm lens to collimate the beam. This makes the beam slightly larger than the aperture (4.8 mm by 3.8 mm) of the camera. Wavelength range of the sensor is 350 - 1100 nm with a spatial resolution of 29.6 µm. There is also a beamsplitter so that the far field image of the beam so that the diffraction limit of the spot is measured. The PHASICS camera is connected to a laptop to analyze the wavefronts and in the future implement the phase correction. Figure 2 actual shows the arrangement in the laboratory to date.

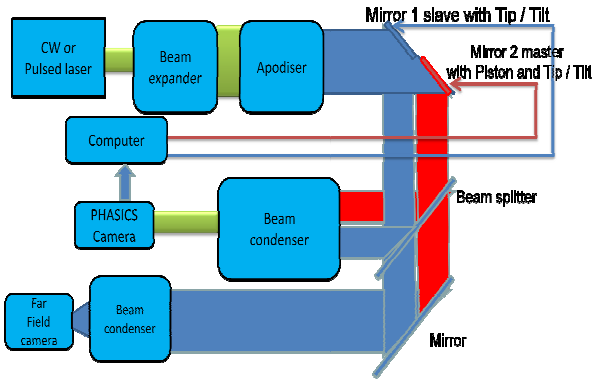

Figure 1. Experimental layout.

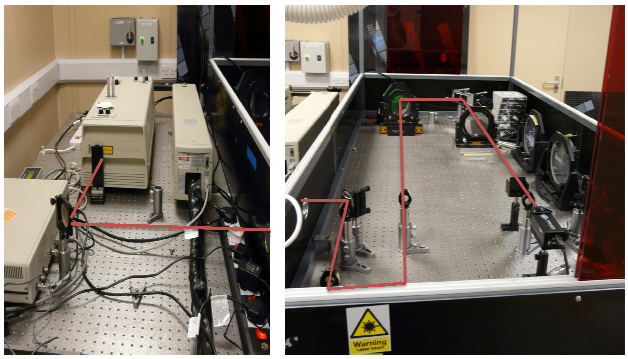

Figure 2. Laboratory setup, beam path is shown by the use of the red line.

The current PHASICS software on the laptop displays the two subbeam wavefront measurement plus interference between the two subbeams. The interference area can adjusted by varying distance between the grating and the CCD sensor up to a maximum. The distance is defined by the beam parameters and the distance that separates the two beams. An algorithm is then employed to calculate the difference in phase between the two beams, which is displayed as a fraction of the wavelength being measured. This is carried out by the use of Legendre polynomials as opposed to Zernike polynomials due to the fact that the wavefronts are square. The wavefronts can be measured with the use of Zernike polynomials by defining the area as circular in the software. The piston and discrete Tip / Tilt errors does not yet go to the translation stage and their respective stages. With the purchase of a programming language from PHASCIS, which will gives us access to the analyzing software and then it will be possible to introduce a feedback loop to control the piston error and the discrete Tip / Tilt, which is what we are planning to do in the immediate future.
This consists of a Ti:Sapphire Tsunami working from 0.8 to 1.1 µm, 100 fs pulses at 80 MHz pulse rep rate.

Future Developments

This project is funded by the LASERLAB-EUROPE II fund.

We will develop the system for analyzing the wavefront for a feedback control system, so that the two beams will be locked spatial. This will initially be carried out on a two beam system, which will be expanded to a four beam system. This will require further mirrors and a different configuration to arrange the mirrors. We also require further development of the software so that three of the mirrors receive error signals to spatial overlap them.

We would like to implement a basic interferometer system so that an estimation of the distance between n numbers of mirrors can be calculated in the first instance. In which the PHASICS

camera can then finely adjust the n numbers of mirrors in the system.

Once the system is in a working state and fully tested in the HAPPIE laboratory then we would like to develop the system on the Astra-Gemini laser system here at CLF, to spatial overlap the two beams.

We also like to explore techniques to temporal lock several beams together.

Conclusions

We have a setup in the HAPPIE laboratory with the current technology to carry out analyses of subbeams wavefront to spatial phase them. In the future we are going to design a feedback system so that the two beams are permanently spatial locked after this we would implement the system on Astra-Gemini.

We are also going to explore experimentally the temporal locking two picoseconds pulses in the future.

References

1. A high power laser fusion facility for Europe" Nature Physics, Vol 2, Jan. 2006
2. "Shack-Hartmann sensor for the active phasing experiment" Proc. SPIE 6267, 626730,(2006)
3. "Theoretical description of Shack-Hartmann wavefront sensor" Optics Communication 222 (2003) 81-92
4. "Single-shot wavefront measurements of high intensity ultrashort laser pulses with a three wave inteferoemeter" Optics Letters Vol. 23 No.8 1998
5. "Overview of PETAL, multi-Petawatt project on the LIL facility", Plasma Physics and controlled Fusion, 50, (2008)124045
6. "Piston measurement by quadriwave lateral shearing interferometry" Optics Letters, Vol.31, No. 17 September 1, 2006